Short communication

Effect of operating conditions on carbon corrosion in polymer electrolyte membrane fuel cells

Katie Heeyum Lim[a], Hyung-Suk Oh[a], Sang-Eun Jang[a], Young-Jin Ko[a], Hyun-Jong Kim[b], Hansung Kim[a,*]

[a] Dept. of Chemical and Biomolecular Engineering, Yonsei University, 134 Shinchon-Dong, Seodaemun-gu, 120-749 Seoul, Republic of Korea
[b] Korea Institute of Industrial Technology (KITECH), Songo-Dong, Yeonsu-Gu, Incheon, Republic of Korea
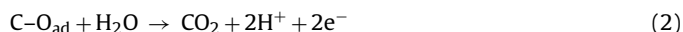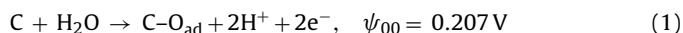
ABSTRACT

The influence of humidity, cell temperature and gas-phase O_2 on the electrochemical corrosion of carbon in polymer electrolyte membrane fuel cells is investigated by measuring CO_2 emission at a constant potential of 1.4 V for 30 min using on-line mass spectrometry. Carbon corrosion shows a strong positive correlation with humidity and cell temperature. The presence of water is indispensable for electrochemical carbon corrosion. By contrast, the presence of gas-phase O_2 has little effect on electrochemical carbon corrosion. With increased carbon corrosion, changes in fuel cell electrochemical characteristics become more prominent and thereby indicate that such corrosion significantly affects fuel cell durability.

© 2009 Elsevier B.V. All rights reserved.

1. Introduction

Attention has been devoted to the electrochemical corrosion of carbon used as a catalyst support because this is considered to be one of the key factors limiting the durability of polymer electrolyte membrane fuel cells (PEMFCs) [1–3]. The reported mechanism of carbon corrosion suggests that functional oxygen groups are generated on the carbon surface above 0.207 V vs. SHE upon contact with water (Eq. (1)), and are in turn converted to CO_2 (Eq. (2)) at high overpotential [4]:

$$C + H_2O \rightarrow C{-}O_{ad} + 2H^+ + 2e^-, \quad \psi_{00} = 0.207\,V \tag{1}$$

$$C{-}O_{ad} + H_2O \rightarrow CO_2 + 2H^+ + 2e^- \tag{2}$$

This implies that the electrochemical kinetics of carbon corrosion are slow. Thus, no severe carbon corrosion is observed under normal conditions of PEMFC operation. On the other hand, the rate of corrosion accelerates especially during repetitive start-up/shut-down operations because of the reverse current phenomenon [5,6]. It is well known that the air|fuel boundary at the anode increases the cathodic potential to a level higher than the open-circuit voltage. Such a high potential quickly corrodes the carbon catalyst support and results in rapid degradation of fuel cell performance.

In the mechanism of electrochemical carbon corrosion described above, CO_2 is a final product and the source of oxygen for

CO_2 formation is water. However, published efforts to explain the effect of water on carbon corrosion are contradictory. Maass et al. [4] and Stevens et al. [7] reported that carbon corrosion becomes more extensive as relative humidity increases. On the other hand, Borup et al. [8] found that carbon corrosion increases with decreasing relative humidity. This discrepancy may result from the unreliability of methods used to estimate the degree of carbon corrosion. They determined carbon corrosion by weight difference, or by changes in the ratios of Pt and carbon signals measured by X-ray diffraction (XRD) before and after corrosion tests. Both these methods are indirect measurements of carbon corrosion because data are affected by changes in the amounts of both carbon and platinum. Cyclic voltammetry (CV) tests are also widely used to investigate carbon corrosion [9–11]. Using CV, the amounts of surface oxides generated on a carbon surface are quantified by integrating peak areas below the curve corresponding to the positive-going scan, after subtracting the double-layer charge. However, surface oxides can be oxidized further into carbon dioxide gas, which cannot be detected by CV at elevated temperature or in the presence of Pt [12]. Therefore, CV does not quantify the electro-oxidation of carbon in a systematic manner. With these concerns in mind, mass spectrometry [13,14] and non-dispersive infrared spectrometry [4] have recently been introduced to evaluate carbon corrosion, by measuring CO_2 concentration, which is direct evidence of carbon corrosion. Thus, the newer techniques offer advantages in comparison with previously employed approaches.

The focus of this work is to obtain a further understanding of electrochemical carbon oxidation in PEMFCs. The influence of humidification, cell temperature and the presence of gas-phase

---

oxygen is studied systematically using on-line mass spectrometry and several electrochemical techniques.

2. Experimental

In this study, Pt/C catalysts from Johnson Mathey Co. (40 wt.% Pt) were used for both the cathode and the anode. The catalysts were ultrasonically mixed with 5 wt.% Nafion ionomer in isopropanol and then sprayed directly on a Nafion 212 membrane to the prepare membrane electrode assemblies (MEAs). The cell area was 5 cm^2 and the amount of Pt loaded was 0.4 mg cm^{-2}.

Several electrochemical experiments were carried out before and after corrosion tests to examine physical and electrochemical changes associated with carbon corrosion. Polarization curves were obtained at a cell temperature of 75 °C under ambient pressure, with O_2 at the cathode and H_2 at the anode. After the corrosion test, the MEAs were reactivated so that the performance reached the steady state. Impedance measurements were performed at 0.8 V to measure the membrane and the charge-transfer resistance. Cyclic voltammetry was performed in the range of 0.05–1.2 V at a sweep rate of 50 mV s^{-1} to determine the electrochemically active Pt surface area. Prior to CV, the cathode was purged with nitrogen gas for 40 min to remove oxygen. After completion of CV, carbon-corrosion experiments were conducted under various conditions. Humidified H_2 was supplied to the anode at a flow rate of 20 cm^3 and N_2 or O_2 gases at varying humidity were supplied to the cathode at a flow rate of 30 cm^3. A constant potential of 1.4 V with reference to the anode was applied to the cathode of the fuel cell for 30 min and the amount of CO_2 produced was monitored as a function of time using on-line mass spectrometry. During the corrosion test, the cathode becomes the anode of the externally powered cell and exhibits carbon corrosion, water oxidation and oxidation of Pt. On the other hand, the anode of the fuel cell behaves as both a counter electrode and a reference electrode.

3. Results and discussion

3.1. Effect of humidity on electrochemical carbon corrosion

To investigate the dependence of electrochemical carbon corrosion on humidity, humidified N_2 was passed through saturators at different temperatures and then supplied to the cathode during corrosion tests. The amount of CO_2 emitted was simultaneously measured using on-line mass spectrometry. As can be seen in Fig. 1, mass spectrometry profiles could not be obtained when non-humidified or humidified N_2 was supplied at 30 °C because no CO_2 was detected. This implies that carbon corrosion does not occur under these conditions. When the humidifying temperature increased to 60 °C, however, CO_2 emission was detected as soon as a potential of 1.4 V was applied to the cell. With further increase of the humidifying temperature to 90 °C, the amount of released CO_2 increased significantly. These observations suggest that the amount of water provided to the fuel cell system plays a critical role in the activation of electrochemical carbon corrosion.

The performance of PEMFCs before and after corrosion tests is shown in Fig. 2. When non-humidified N_2 or humidified N_2 at 30 °C was supplied to the cathode during corrosion tests, the performance of the system remained essentially unaltered, whereas cells tested with humidified N_2 at 60 or 90 °C showed considerable performance decays of about 50.7 and 91.3% at 0.6 V, respectively. These results are in good agreement with the mass spectrometry data in Fig. 1. With increase in humidity, carbon corrosion rises, and induces a decrease in the performance of MEAs.

To examine changes in the active surface area of Pt, CV measurements on MEAs were conducted before and after corrosion tests.
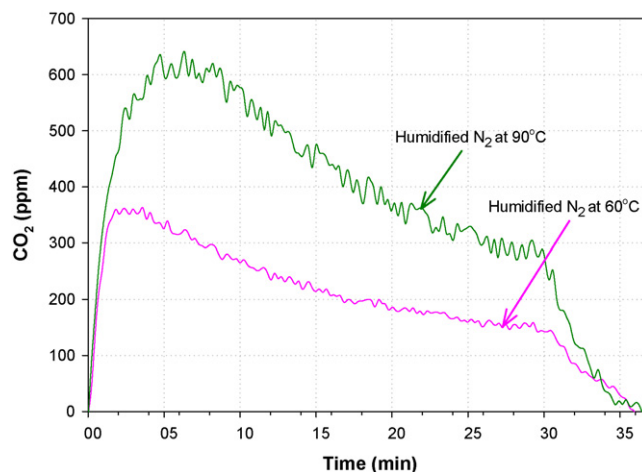

Fig. 1. CO_2 mass-spectrographic profiles of MEAs. Corrosion tests performed at 1.4 V with non-humidified N_2 and humidified N_2 delivered to cathode after passing through saturator at 30, 60 and 90 °C.

As shown in Fig. 3, carbon corrosion was responsible for a severe decrease in the active surface area. With conversion of the carbon support to CO_2 by corrosion, the number of sites for Pt loading falls and thereby forces Pt nanoparticles to aggregate at relatively stable sites. The loss of active surface area may occur by dissolution of Pt [15,16]. A study of Pt dissolution using a quartz crystal microbalance showed that any mass decrease arising from Pt dissolution is not immediately detectable because the mass of the Pt electrode initially increases as a result of oxide layer formation [17]. Under the present experimental conditions, the carbon-corrosion test is performed for only 30 min, which is insufficient time for Pt dissolution to become predominant. In addition, the potential of 1.4 V applied during the corrosion test creates a thick protective oxide layer that reduces the rate of Pt dissolution [17]. Therefore, it is considered that coalescence of Pt particles as a result of carbon corrosion is the principal contributor to the observed decrease in active surface area.

Impedance analyses were performed to examine the effect of carbon corrosion on resistance changes in fuel cells. The experiments were performed at 0.8 V in the frequency range between 0.1 and 1 kHz and the results are presented in Fig. 4. When non-humidified or humidified N_2 is supplied at 30 °C, i.e., under conditions where no carbon corrosion occurred, no distinct changes are detected. On the other hand, both resistances measured in
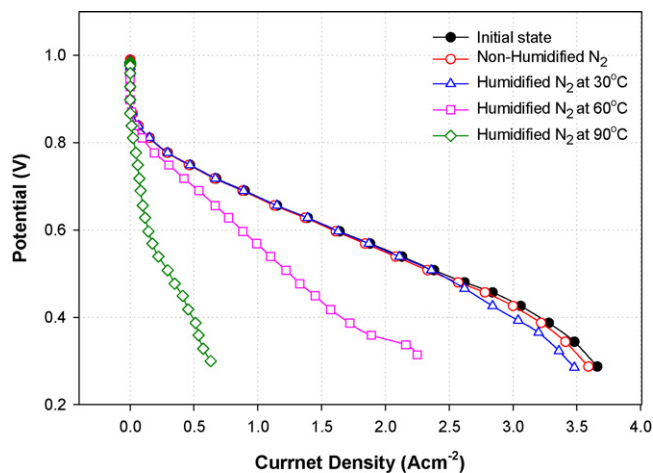

Fig. 2. Comparison of MEA performances before and after corrosion tests using non-humidified N_2 and humidified N_2 at 30, 60 and 90 °C.
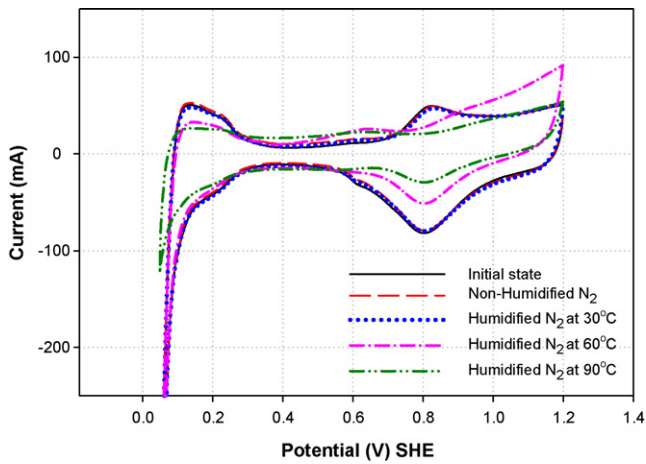
Fig. 3. Cyclic voltammograms of MEAs before and after corrosion tests at scan rate of 50 mV s^{-1}. Corrosion tests performed at 1.4 V with non-humidified N$_2$ and humidified N$_2$ delivered to cathode after passing through saturator at 30, 60 and 90 °C.

the high- and low-frequency regions increased significantly with increase in the humidifying temperature, presumably because of a decrease in the active Pt surface area and an increase in the contact electrode resistance [13]. The experimental results associated with the corrosion tests are summarized in Table 1.

3.2. Effect of temperature on electrochemical carbon corrosion

Mass spectrographs recorded during CO$_2$ formation at different cell temperatures are presented in Fig. 5. During corrosion tests, the water level supplied to the cell is assumed to be constant because the humidifying temperature of N$_2$ is set at 60 °C. When CO$_2$ generation at cell temperatures of 60, 75 and 90 °C are compared, greater carbon corrosion is seen at higher cell temperatures. At a cell temperature of 60 °C, the amount of CO$_2$ at the beginning of the corrosion test for 15 min is negligible, i.e., less than 25 ppm. By contrast MEAs corroding electrochemically at cell temperatures of 75 and 90 °C display considerable increases in CO$_2$ generation, i.e., 145 and 362 ppm, respectively. The MEA performances before and after corrosion tests are shown in Fig. 6. As expected from the mass spectrometry data in Fig. 5, greater falls in MEA performance are observed at higher cell temperatures. Note that the performance of an MEA corroded at a cell temperature of 60 °C is almost equivalent to that of an uncorroded MEA. To confirm the effect of temperature
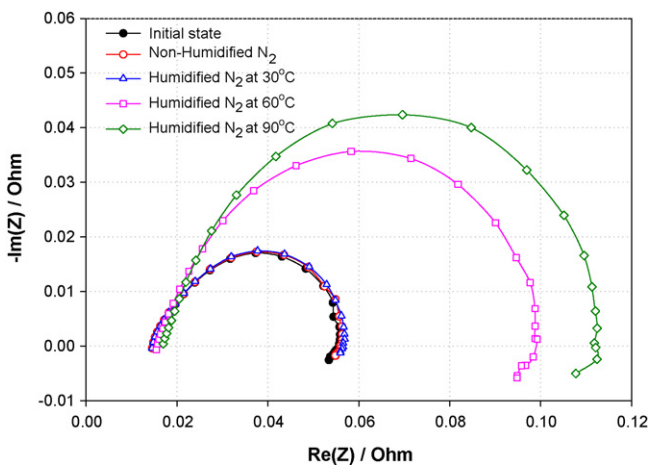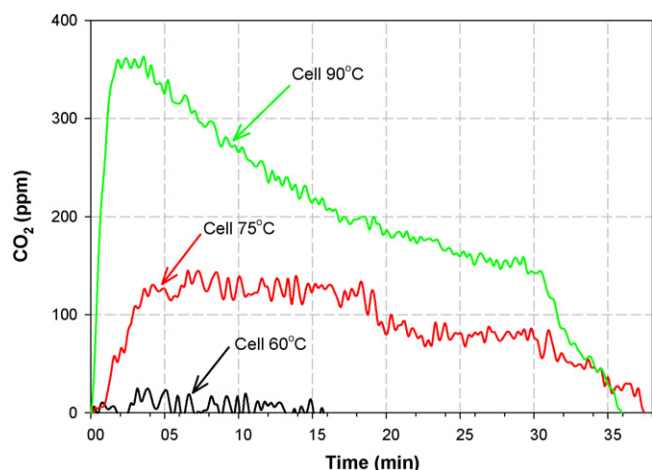

Fig. 4. Nyquist plots of MEAs at 0.8 V before and after corrosion tests using non-humidified N$_2$ and humidified N$_2$ at 30, 60 and 90 °C.

Table 1
Summary of changes before and after corrosion test.

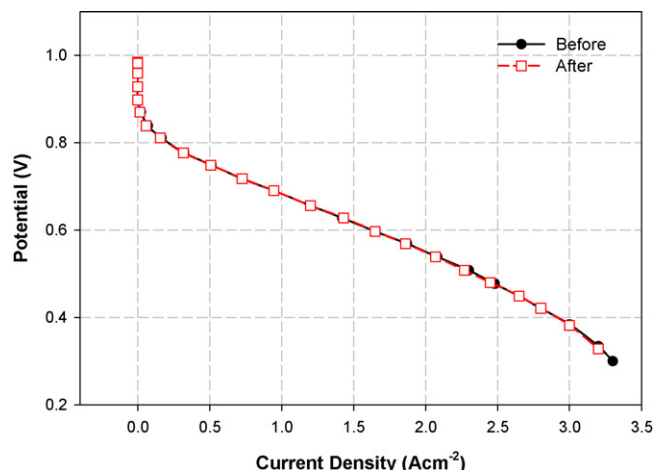| Conditions	MEA performance at 0.6 V (A cm^{-2})		Active surface area (m^2 g^{-1})		Membrane resistance (Ω)		Charge-transfer resistance (Ω)		CO$_2$ production (μL)
	Before	After	Before	After	Before	After	Before	After	1.4 V 30 min
Non-humidified at 90 °C (N$_2$)	1.64	1.63 −0.6%	28.6	28.5 −0.4%	0.014 0%	0.014	0.0413 +0.2%	0.0414	0
Humidified at 30 °C (N$_2$)	1.64 −1.8%	1.61	28.6 −0.4%	28.5	0.014 0%	0.014	0.0413 +1.7%	0.0420	0
Humidified at 60 °C (N$_2$)	1.64 −46.3%	0.88	28.6 −37.8%	17.8	0.014 +10.3%	0.016	0.0413 +100.3%	0.0841	945
Humidified at 90 °C (N$_2$)	1.64 −91.3%	0.14	28.6 −65.7%	9.8	0.014 +17.2%	0.017	0.0413 +130.3%	0.0951	1806

Fig. 5. CO_2 mass-spectrographic profiles of MEAs. Corrosion tests performed at cell temperatures of 60, 75 and 90 °C, with humidified N_2 delivered to cathode after passing through a saturator at 60 °C. Potential fixed at 1.4 V.

Fig. 7. Comparison of MEA performances before and after corrosion tests. Corrosion tests performed at cell temperature of 60 °C with humidified N_2 delivered to cathode after passing through saturator at 90 °C.
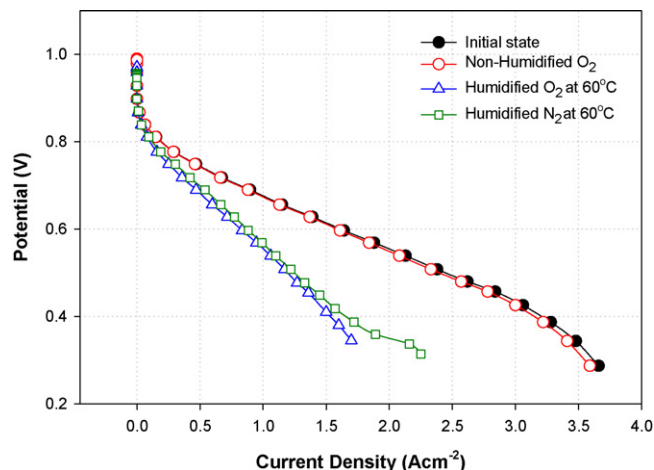
on carbon corrosion, tests were conducted at a cell temperature of 60 °C with humidified N_2 supplied at 90 °C. A comparison of MEA performance before and after the corrosion test is given in Fig. 7 and shows that there is no drop in performance even with high water content and thereby indicates that carbon corrosion is very temperature-sensitive.

### 3.3. Effect of oxygen gas on electrochemical carbon corrosion

It is well known that the presence of gas-phase O_2 contributes to Pt electrochemical surface oxidation resulting in a decrease in electrocatalytic oxygen reduction activity [18,19]. Nevertheless, relatively few studies have explored the influence of gas-phase oxygen on electrochemical carbon corrosion. In this study, non-humidified or humidified O_2 at 60 °C is supplied to the cathode. The cell temperature is held at 90 °C. As shown in Fig. 8, when an MEA is supplied with non-humidified O_2, the performance does not change. Furthermore, the drop in performance on supply of humidified O_2 at 60 °C is similar to that when N_2 humidified at the same temperature is supplied which is included in Fig. 8 for ease of comparison. These results are confirmed by the mass spectrometry data given in Fig. 9. When non-humidified O_2 is supplied,

Fig. 8. Comparison of MEA performances before and after corrosion tests. Corrosion tests performed at cell temperature of 90 °C with cathode-delivered non-humidified O_2 or humidified O_2 after passing through saturator at 60 °C. Performance of MEA after a corrosion test using humidified N_2 passed through saturator at 60 °C is shown for ease of comparison.
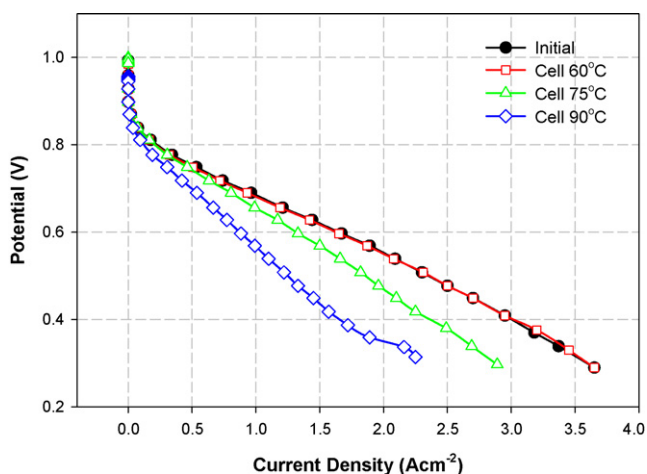
Fig. 6. Comparison of MEA performances before and after corrosion tests. Corrosion tests performed at cell temperatures of 60, 75 and 90 °C, with humidified N_2 delivered to cathode after passing through saturator at 60 °C.
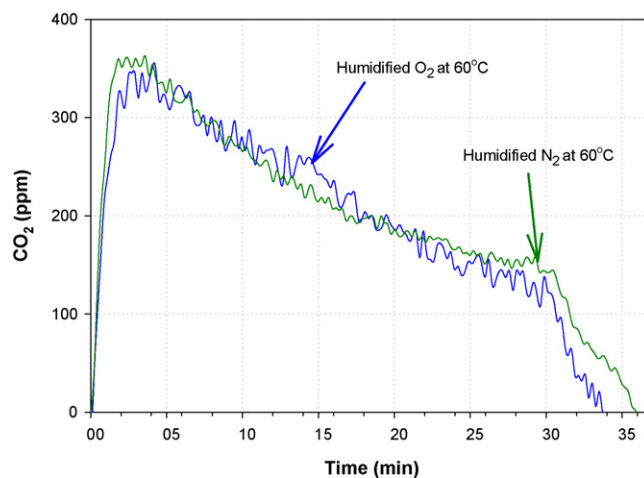
Fig. 9. CO_2 mass-spectrographic profiles of MEAs. Corrosion tests performed at cell temperature of 90 °C with humidified O_2 or N_2 delivered to cathode after passing through saturator at 60 °C. Potential fixed at 1.4 V.

CO$_2$ generation is not detected, as is the case when non-humidified N$_2$ is employed. In agreement with the results described above, at a humidifying temperature of 60 °C, no atmospheric dependence (N$_2$ vs. O$_2$) can be seen in the mass spectra. By contrast, it has been reported that the presence of O$_2$ accelerated carbon corrosion [20]. It was concluded that the chemical reactions of some intermediates existing on carbon surface with O$_2$ accelerate the electrochemical corrosion. However, this phenomenon is not observed in the experiments reported here. If hydrogen peroxide can be formed during an oxygen reduction reaction, it is possible that chemical oxidation of carbon by hydrogen peroxide could form CO$_2$ [4]. From a thermodynamic viewpoint, hydrogen peroxide is not expected to be generated at 1.4 V under the present experimental conditions. Therefore, CO$_2$ generation by a pathway involving hydrogen peroxide can be safely excluded. The results make it clear that electrochemical corrosion of carbon greatly affects fuel cell durability, and that the principal causes of electrochemical corrosion of the carbon support do not include the presence of O$_2$, but are rather the water content in the catalyst layer and the cell temperature.

4. Conclusions

The influence of humidity, cell temperature and gas-phase O$_2$ on the electrochemical corrosion of carbon in PEMFC investigated by measuring CO$_2$ emission using on-line mass spectrometry. Electrochemical carbon corrosion is strongly dependent on humidity and cell temperature, but the presence of gas-phase O$_2$ does not affect corrosion. Carbon corrosion is accelerated on increasing the humidity and raising the cell temperature. Under humidified conditions, a cell temperature over 60 °C is required for electrochemical carbon corrosion.

References

[1] E. Antolini, J. Mater. Sci. 38 (2003) 2995–3005.
[2] X. Cheng, L. Chen, C. Peng, Z.W. Chen, Y. Zhang, Q.B. Fan, J. Electrochem. Soc. 151 (2004) A48–A52.
[3] J. Willsau, J. Heitbaum, J. Electroanal. Chem. 161 (1984) 93–101.
[4] S. Maass, F. Finsterwalder, G. Frank, R. Hartmann, C. Merten, J. Power Sources 176 (2008) 444–451.
[5] C.A. Reiser, L. Bregoli, T.W. Patterson, J.S. Yi, J.D. Yang, M.L. Perry, T.D. Jarvi, Electrochem. Solid State Lett. 8 (2005) A273–A276.
[6] H. Tang, Z. Qi, M. Ramani, J.F. Elter, J. Power Sources 158 (2006) 1306–1312.
[7] D.A. Stevens, M.T. Hicks, G.M. Haugen, J.R. Dahn, J. Electrochem. Soc. 152 (2005) A2309–A2315.
[8] R.L. Borup, J.R. Davey, F.H. Garzon, D.L. Wood, M.A. Inbody, J. Power Sources 163 (2006) 76–81.
[9] J. Wang, G. Yin, Y. Shao, Z. Wang, Y. Gao, J. Power Sources 176 (2008) 128–131.
[10] L. Li, Y. Xing, J. Electrochem. Soc. 153 (2006) A1823–A1828.
[11] J. Wang, G. Yin, Y. Shao, S. Zhang, Z. Wang, Y. Gao, J. Power Sources 171 (2007) 331–339.
[12] L. Li, Y. Xing, J. Power Sources 178 (2008) 75–79.
[13] H.S. Oh, J.G. Oh, S. Haam, K. Arunabha, B. Roh, I. Hwang, H. Kim, Electrochem. Commun. 10 (2008) 1048–1051.
[14] L.M. Roen, C.H. Paik, T.D. Jarvi, Electrochem. Solid State Lett. 7 (2004) A19–A22.
[15] X. Wang, R. Kumar, D.J. Myers, Electrochem. Solid State Lett. 9 (2006) A225–A227.
[16] P.J. Ferreira, G.J. La O, Y. Shao-Horn, D. Morgan, R. Makharia, S. Kocha, H.A. Gasteiger, J. Electrochem. Soc. 152 (2005) A2256–A2271.
[17] V.A.T. Dam, F.A. de Bruijn, J. Electrochem. Soc. 154 (2007) B494–B499.
[18] A. Damjanovic, J. Electrochem. Soc. 138 (1991) 2315–2320.
[19] A. Damjanovic, P.G. Hudson, J. Electrochem. Soc. 135 (1988) 2269–2273.
[20] Z. Siroma, J. Tanaka, K. Yasuda, K. Tanimoto, M. Inaba, A. Tasaka, Electrochemistry 75 (2007) 258–260.